Natural Frequencies of Bending and Torsion Stiff Composite Conical Shells with Delamination

Sudip Dey, Amit Karmakar

Abstract

Extensive uses of composite structures can be found in weight-sensitive structural applications due to its high specific strength and high specific stiffness. Laminated composite shallow conical shell with low aspect ratio can be idealized as turbomachinery blades. Delamination or inter-laminar debonding is the most feared damage mode in composites. This paper presents a finite element method to investigate the effects of delamination on free vibration characteristics of eight layered graphite-epoxy composite pre-twisted conical shells with bending stiff and torsion stiff configurations. The formulation is based on eight noded isoparametric plate bending element applying Mindlin's theory and neglecting Coriolis effect for moderate rotational speeds. The Multi-point Constraint algorithm is employed to ensure the compatibility of deformation and equilibrium of resultant forces and moments at the delamination crack front. The QR iteration algorithm is utilized to solve the standard eigen value problem. Finite element codes are developed to obtain the numerical results concerning the effects of twist angles and rotational speeds. Numerical results obtained for eight layered bending stiff and torsion stiff laminates with mid-plane delamination are the first known non-dimensional frequencies for the type of analyses carried out here.

Keywords: Finite Element, Delamination, Conical Shell, Bending Stiff, Torsion Stiff, Multi-point Constraint

1 Introduction

Composite materials are advantageous due to its high stiffness to weight ratio. Laminated composite structures have wide range of weight sensitive applications such as in aircrafts, naval ships, space vehicles and other high performance applications. Rotating twisted composite conical shells (Figure 1) with low aspect ratio can be idealized as turbo-machinery blades. Delamination is the most feared damage mode which may occur due to manufacturing defects or in-service condition. The laminated composite structures with delamination exhibit new vibration frequencies depending on the size and location of delamination. The presence of invisible delamination can be detected with the help of prior knowledge of natural frequencies for delaminated composite laminates. In order to ensure the safety of operation, a profound understanding of dynamic characteristics of composite laminates is essential for the designers. The first established work on pretwisted composite plates was carried out by Qatu et al. [1] to determine the natural

Sudip Dey (Corresponding author)
Mechanical Engineering Department, Jadavpur University, Kolkata – 700 032, India,
E-mail: infosudip@gmail.com

Amit Karmakar
Mechanical Engineering Department, Jadavpur University, Kolkata – 700 032, India,
E-mail: shrikatha@yahoo.co.in

frequencies of stationary plates using laminated shallow shell theory using Ritz method. Liew et al. [2] investigated on pretwisted conical shell to find out the vibratory characteristics of stationary conical shell by using Ritz procedure and by using the same method, the first known three dimensional continuum vibration analysis including full geometric non-linearities and centrifugal accelerations in composite blades was carried out by McGee and Chu [3]. Regarding delamination model, two worth mentioning investigations were carried out. It included analytical and experimental determination of natural frequencies of delaminated composite beam by Shen and Grady [4] and the second one dealt with finite element treatment of the delaminated composite cantilever beam and plate by Krawczuk et al. [5] for free vibration analyses. There is not only significant work incurred on single delamination, but also on multiple delamination. Considering multiple delamination, failure analysis of composite plate due to bending and impact was numerically investigated by Parhi et al. [6] using finite element method. To ensure the compatibility of deformation and equilibrium of resultant forces and moments at the delamination crack front a multi-point constraint algorithm [7] is incorporated which leads to anti-symmetric element stiffness matrices. QR iteration algorithm [8] is utilized to solve the standard eigenvalue problem.

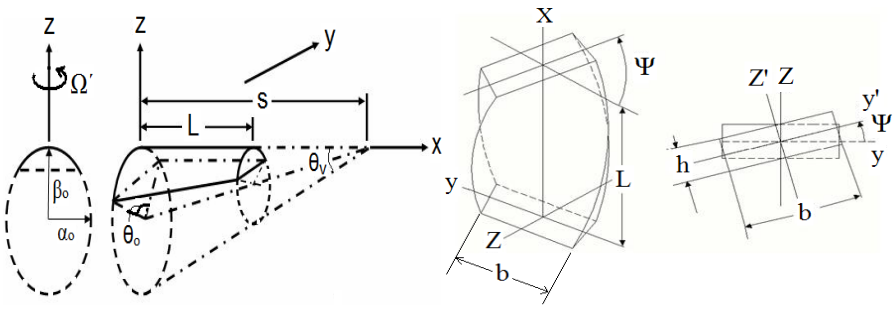

(a) (b)

Figure 1: Geometry of (a) untwisted conical shell and (b) twisted plate

A review of open literature on composite shells reveals that the study on free vibration of delaminated conical shells is far from complete. This paper presents a finite element based numerical approach to determine the non-dimensional natural frequencies of graphite-epoxy composite conical shells with bending stiff and torsion stiff configuration neglecting effect of dynamic contact between delaminated layers.

2 Theoretical Formulation

A shallow shell is characterized by its middle surface which is defined by the equation [9],

$$z = -\frac{1}{2}\left[\frac{x^2}{R_x} + 2\frac{xy}{R_{xy}} + \frac{y^2}{R_y}\right] \qquad (1)$$

where R_x and R_y denote the radii of curvature in the x and y directions, respectively. The radius of twist (R_{xy}), length (L) of shell and twist angle (Ψ) are related as,

$$\tan \psi = - \frac{L}{R_{xy}} \tag{2}$$

The dynamic equilibrium equation for moderate rotational speeds neglecting Coriolis effect is derived employing Lagrange's equation of motion and equation in global form is expressed as [10],

$$[M] \{ \ddot{\delta} \} + ([K] + [K_\sigma]) \{\delta\} = \{F(\Omega^2)\} \tag{3}$$

where [M], [K], $[K_\sigma]$ are global mass, elastic stiffness and geometric stiffness matrices, respectively. $\{F(\Omega^2)\}$ is the nodal equivalent centrifugal forces and $\{\delta\}$ is the global displacement vector. $[K_\sigma]$ depends on the initial stress distribution and is obtained by the iterative procedure [11] upon solving,

$$([K] + [K_\sigma]) \{\delta\} = \{F(\Omega^2)\} \tag{4}$$

The natural frequencies (ω) are determined from the standard eigenvalue problem [8] which is represented below and is solved by the QR iteration algorithm,

$$[A] \{\delta\} = \lambda \{\delta\} \tag{5}$$
$$[A] = ([K] + [K_\sigma])^{-1} [M] \tag{6}$$
$$\lambda = 1/ \omega_n^2 \tag{7}$$

2.1 Multi-point constraint

Figure 2 represents the cross-sectional view of a typical delamination crack tip where nodes of three plate elements meet together to form a common node. The undelaminated region is modelled by plate element 1 of thickness h, and the delaminated region is modeled by plate elements 2 and 3 whose interface contains the delamination (h_2 and h_3 are thicknesses of elements 2 and 3 respectively). The elements 1, 2 and 3 are freely allowed to deform prior to imposition of the constraints conditions. Nodal displacements of elements 2 and 3 at crack tip [7],

$$u_j = u'_j - (z - z'_j) \theta_{xj} \tag{8}$$
$$v_j = v'_j - (z - z'_j) \theta_{yj} \tag{9}$$
$$w_j = w'_j \quad \text{(where, } j = 2, 3) \tag{10}$$

where u'_j , v'_j and w'_j are the mid-plane displacements and z'_j is the z-coordinate of mid-plane of element j and θ_x , θ_y are the rotations about x and y axes, respectively. The above equation also holds good for element 1 and z'_1 equal to zero. The transverse displacements and rotations at a common node have values expressed as,

$$w_1 = w_2 = w_3 = w \tag{11}$$
$$\theta_{x1} = \theta_{x2} = \theta_{x3} = \theta_x \tag{12}$$
$$\theta_{y1} = \theta_{y2} = \theta_{y3} = \theta_y \tag{13}$$

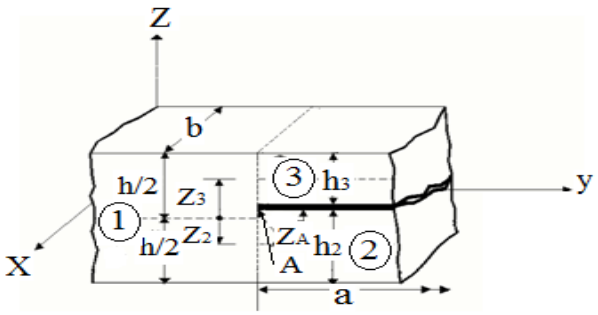

Figure 2: Plate elements at a delamination crack tip

In-plane displacements of all three elements at crack tip are equal and they are related as [7],

$$u'_2 = u'_1 - z'_2\,\theta_x \quad (14)$$

$$v'_2 = v'_1 - z'_2\,\theta_y \quad (15)$$

$$u'_3 = u'_1 - z'_3\,\theta_x \quad (16)$$

$$v'_3 = v'_1 - z'_3\,\theta_y \quad (17)$$

where u'_1 is the mid-plane displacement of element 1. Equations of (11) to (17) relating the nodal displacements and rotations of elements 1, 2 and 3 at the delamination crack tip, are the multipoint constraint equations used in finite element formulation to satisfy the compatibility of displacements and rotations. Mid-plane strains between elements 2 and 3 are related as [7],

$$\{\varepsilon'\}_j = \{\varepsilon'\}_1 + z'_j\,\{k\} \quad (18)$$

where $\{\varepsilon\}$ represents the strain vector and $\{k\}$ is the curvature vector being identical at the crack tip for elements 2 and 3. This equation can be considered as a special case for element 1 and z'_1 is equal to zero. In-plane stress-resultants, $\{N\}$ and moment resultants, $\{M\}$ of elements 2 and 3 can be expressed as,

$$\{N\}_j = [A]_j\,\{\varepsilon'\}_1 + (z'_j\,[A]_j + [B]_j)\,\{k\} \quad \text{(where } j = 2, 3) \quad (19)$$

$$\{M\}_j = [B]_j\,\{\varepsilon'\}_1 + (z'_j\,[B]_j + [D]_j)\,\{k\} \quad \text{(where } j = 2, 3) \quad (20)$$

where [A], [B] and [D] are the extension, bending-extension coupling and bending stiffness coefficients of the composite laminate, respectively. Thus the formulation based on the multi-point constraints condition leads to unsymmetric stiffness matrix. The resultant forces and moments at the delamination front for the elements 1, 2 and 3 satisfy the following equilibrium conditions,

$$\{N\} = \{N\}_1 = \{N\}_2 + \{N\}_3 \quad (21)$$

$$\{M\} = \{M\}_1 = \{M\}_2 + \{M\}_3 + z'_2\,\{N\}_2 + z'_3\,\{N\}_3 \quad (22)$$

$$\{Q\} = \{Q\}_1 = \{Q\}_2 + \{Q\}_3 \quad (23)$$

where {Q} denotes the transverse shear resultants.

3 Results and Discussion

Non-dimensional natural frequencies for conical shells ($R_x=\infty$) having a square plan-form ($L/b_o=1$), curvature ratio (b_o/R_y) of 0.5 and thickness ratio (s/h) of 1000 are obtained corresponding to different speeds of rotation Ω = 0.0, 0.5 and 1.0 (where $\Omega=\Omega'/\omega_o$) and relative distance, d/L=0.33, 0.5 and 0.66, considering three different angles of twist, namely ψ=15°, 30° and 45°, in addition to the untwisted one (ψ=0°). The parameters n, Ω', ω_o, ρ, L, b_o, h, d, a, θ_v and θ_o represent the number of layers, actual angular speed of rotation, fundamental natural frequency of a non-rotating shell, density, length, reference width, thickness, distance of the centerline of delamination from the clamped (fixed) end, crack length, vertex angle and base subtended angle of cone, respectively. The finite element formulation employs eight noded isoparametric plate bending element with five degrees of freedom at each node. Material properties of graphite-epoxy composite [12] considered as E_1=138.0 GPa, E_2=8.96 GPa, ν=0.3, G_{12}=7.1 GPa, G_{13}=7.1 GPa, G_{23}=2.84 GPa.

3.1 Validation

Computer codes are developed based on present finite element method followed by convergence studies. The numerical results obtained are compared and validated with the results of published literature [2, 11] as furnished in Table 1 and Table 2. The numerical results show an excellent agreement with the previously published results and demonstrate the capability and accuracy of the computer codes.

Table 1: Convergence Study for NDFF [$\lambda = \omega_n b_o^2 \sqrt{(\rho h/D)}$] for graphite-epoxy composite pretwisted shallow conical shell considering ν=0.3, L/s=0.7, s/h=1000, θ_v=15° and θ_o=30°

Ψ	*Aspect Ratio(L/s)*	*Present FEM (8x8)*	*Present FEM (6x6)*	*Liew et al. [2]*
0°	*0.6*	*0.3524*	*0.3552*	*0.3599*
	0.7	*0.2991*	*0.3013*	*0.3060*
	0.8	*0.2715*	*0.2741*	*0.2783*
30°	*0.6*	*0.2805*	*0.2834*	*0.2882*
	0.7	*0.2507*	*0.2528*	*0.2575*
	0.8	*0.2364*	*0.2389*	*0.2417*

Table 2: NDFF of graphite-epoxy composite isotropic rotating cantilever plate, considering L/b=1, h/L=0.12, $D=Eh^3/\{12(1-\nu^2)\}$, ν =0.3

Ω	*Present FEM*	*Sreenivasamurthy et al.[11]*
0.0	*3.4174*	*3.4368*
0.4	*3.7110*	*3.7528*
0.8	*4.4690*	*4.5678*

3.2 Effect of twist and rotation across thickness

From Table 3, it is observed that at stationary condition, non-dimensional fundamental natural frequencies (NDFF) of both bending stiff and torsion stiff configurations attained maximum values for twist angle ψ=0° and gradually decreased to a minimum value for twist angle ψ=45°. It is also observed that delaminated NDFF are found lower than undelaminated (ND) one at stationary condition irrespective of twist angle. In general, at stationary condition, NDFF decreases with the increase of twist angle for both delaminated and undelaminated bending and torsion stiff configurations. At rotating condition, NDFF of delaminated bending stiff composite conical shell found drooping trend with the increase of twist angle, while a typical trend is exhibited with increase of twist angle for torsion stiff configuration. The centrifugal stiffening effect (i.e., increase of structural stiffness with increase of rotational speed) is predominantly found with reference to NDFF of bending stiff composites irrespective of twist angle, while the same is not identified for torsion stiff except for ψ=15°.

Table 3: NDFF [$\omega = \omega_n L^2 \sqrt{(\rho/E_1 h^2)}$] of graphite-epoxy composite conical shells with mid-plane delamination, considering n=8, h=0.0004, a/L=0.33, d/L=0.5, s/h=1000, L/s=0.7, θ_o=45°, θ_v=20°.

Bending Stiff (0°/0°/30°/-30°)s					*Torsion Stiff (45°/-45°/45°/-45°)s*			
Ψ	*ND*	*With Delamination*			*ND*	*With Delamination*		
		Ω=0.0	*Ω=0.5*	*Ω=1.0*		*Ω=0.0*	*Ω=0.5*	*Ω=1.0*
0°	*0.4149*	*0.3925*	*0.5231*	*0.6015*	*0.2454*	*0.2453*	*0.4168*	*0.2778*
15°	*0.2476*	*0.2378*	*0.4552*	*0.5584*	*0.2126*	*0.2108*	*0.2540*	*0.3587*
30°	*0.1490*	*0.1434*	*0.2617*	*0.4863*	*0.1535*	*0.1508*	*0.2081*	*0.0648*
45°	*0.0975*	*0.0947*	*0.2056*	*0.3641*	*0.0985*	*0.0964*	*0.3159*	*0.2768*

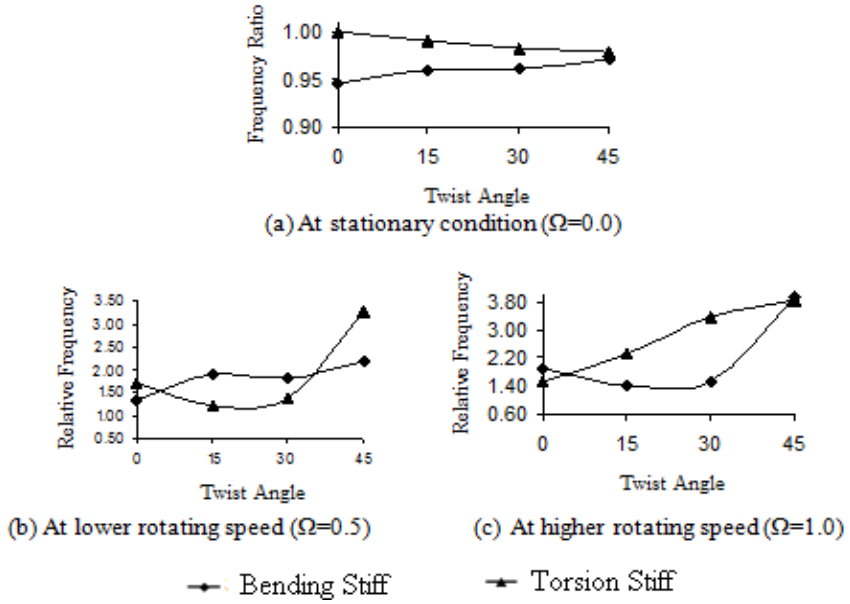

Figure 3: Frequency Ratio and Relative Frequencies at Ω=0.5 and 1.0 for different twist angles of graphite-epoxy composite conical shells with delamination, n=8, h=0.0004, a/L=0.33, d/L=0.5, s/h=1000, L/s=0.7, θ_o=45°, θ_v=20°.

3.3 Effect of frequency ratio and relative frequency

The trend of frequency ratio (ratio of delaminated and undelaminated NDFF) and relative frequencies (ratio of rotating NDFF and stationary NDFF) at Ω=0.5, 1.0 are furnished in Fig. 3 with respect to Table 3. At stationary condition, it is noted that the percentage difference between maximum and minimum frequency ratios found to be 2.6% and 2.1% for bending stiff and torsion stiff, respectively. At Ω=0.5, it is identified that percentage differences between maximum and minimum relative frequencies are found 38.6% and 63.2% for bending stiff and torsion stiff, respectively. At Ω=1.0, percentage differences between maximum and minimum relative frequencies are found 60.1% and 85.0% for bending stiff and torsion stiff, respectively. Hence it leads to the fact that for bending stiff, relative frequencies have pronounced effect for higher rotating speed while the same is also observed for torsion stiff with higher percentage difference compared to bending stiff.

3.4 Effect of twist and rotation along span

From Table 4 and 5, at stationary condition NDFF is observed to decrease with the increase of twist angle for both configurations. For both cases at stationary condition, NDFF is found to increase as the delamination moves towards the free end. It is observed that with d/L=0.33, 0.67 at rotating condition, NDFF decreases with increase of twist angle for bending stiff configuration except for ψ=30° at Ω=1.0. In contrast, for torsion stiff, the same is found to decrease with increase of twist angle, except for ψ=30° (at d/L=0.33 with Ω=0.5, 1.0 and at d/L=0.67 with Ω=0.5). It is

also observed that the centrifugal stiffening effect is predominant with respect to NDFF in case of ψ=15° for both bending stiff and torsion stiff configurations.

Table 4: NDFF [$\omega = \omega_n L^2 \sqrt{(\rho/E_1 h^2)}$] of graphite-epoxy bending stiff conical shells with delamination along span, considering n=8, h=0.0004, a/L=0.33, d/L=0.5, s/h=1000, L/s=0.7, θ_o=45°, θ_v=20°.

ψ	*d/L=0.33*			*d/L=0.67*		
	Ω=*0.0*	Ω=*0.5*	Ω=*1.0*	Ω=*0.0*	Ω=*0.5*	Ω=*1.0*
0°	*0.3902*	*0.5223*	*0.6004*	*0.4015*	*0.5243*	*0.6041*
15°	*0.2339*	*0.4760*	*0.5136*	*0.2418*	*0.4310*	*0.4470*
30°	*0.1390*	*0.3689*	*0.1826*	*0.1450*	*0.1929*	*0.5854*
45°	*0.0911*	*0.2227*	*0.3786*	*0.0947*	*0.1799*	*0.3431*

Table 5: NDFF [$\omega = \omega_n L^2 \sqrt{(\rho/E_1 h^2)}$] of graphite-epoxy torsion stiff conical shells with delamination along span, considering n=8, h=0.0004, a/L=0.33, d/L=0.5, s/h=1000, L/s=0.7, θ_o=45°, θ_v=20°.

Ψ	*d/L=0.33*			*d/L=0.67*		
	Ω=*0.0*	Ω=*0.5*	Ω=*1.0*	Ω=*0.0*	Ω=*0.5*	Ω=*1.0*
0°	*0.2451*	*0.4180*	*0.2806*	*0.2453*	*0.4096*	*0.2761*
15°	*0.2082*	*0.3202*	*0.3582*	*0.2117*	*0.2663*	*0.3524*
30°	*0.1472*	*0.2288*	*0.2430*	*0.1521*	*0.1650*	*0.2816*
45°	*0.0941*	*0.3173*	*0.2876*	*0.0972*	*0.2430*	*0.2604*

4 Conclusions

At stationary condition, NDFF decreases with increase of twist angle for both delaminated and undelaminated bending stiff and torsion stiff configurations. At rotating condition, NDFF of delaminated bending stiff composite is found to decrease with increase of twist angle, while a typical trend is exhibited with increase of twist angle for torsion stiff configuration. In both cases, NDFF is found to increase as delamination moves towards the free end. The results obtained can be considered as reference solutions for the future investigators.

References

[1] M. S. Qatu and A. W. Leissa, "Vibration studies for Laminated Composite Twisted Cantilever Plates", *International Journal of Mechanical Sciences*, vol.33, pp.927-940, 1991.

[2] K. M. Liew, C. M. Lim and L. S. Ong, "Vibration of pretwisted cantilever shallow conical shells", *International Journal of Solids Structures*, vol.31, pp.2463-74, 1994.

[3] O. G. McGee and H. R. Chu, "Three-Dimensional Vibration Analysis of Rotating Laminated Composite Blades", *Journal of Engineering for Gas Turbines and Power*, ASME, vol.116, pp.663–671, 1994.

[4] M. H. H. Shen and J. E. Grady, "Free Vibrations of Delaminated Beams", *Journal of AIAA*, vol.30, pp.1361–1370, 1992.

[5] M. Krawczuk, W. Ostachowicz and A. Zak, "Dynamics of Cracked Composite Material Structures", *Journal of Computational Mechanics*, vol.20, pp.79-83, 1997.
[6] P. K. Parhi, S. K. Bhattacharyya and P. K. Sinha,"Failure analysis of multiple delaminated due to bending and impact"*Bull. Mater. Sci.,*24, pp.143–149, 2001.
[7] C. K. Gim, "Plate Finite Element Modelling of Laminated Plates", *Journal of Composite Structures*, vol.52, pp.157-168, 1994.
[8] K. J. Bathe, *"Finite Element Procedures"*, PHI, New Delhi, 1990.
[9] A.W.Leissa, J.K.Lee and A.J.Wang, "Vibrations of Twisted Rotating Blades", *Journal of Vibration Acoustics, Stress, and Reliability in Design*, vol.106, pp.251-257, 1984.
[10] A. Karmakar and P. K. Sinha, "Failure Analysis of Laminated Composite Pretwisted Rotating Plates", *Journal of Reinforced Plastics and Composites,* vol. 20, pp.1326-1357, 2001.
[11] S. Sreenivasamurthy and V. Ramamurti, "Coriolis Effect on the Vibration of Flat Rotating Low Aspect Ratio Cantilever Plates", *Journal of Strain Analysis*, vol.16, pp. 97-106, 1981.
[12] M. S. Qatu and A. W. Leissa, "Natural Frequencies for Cantilevered Doubly-Curved Laminated Composite Shallow Shells", *Journal of Composite Structures*, vol.17, pp.227-255, 1991.